AN EXPERIMENTAL STUDY OF ACOUSTICALLY INDUCED

ROCKING MOTION OF SIMPLE ASYMMETRIC GEOMETRIES

A Thesis
Presented to
The Academic Faculty

by

Gwendolyn Rodgers

In Partial Fulfillment
of the Requirements for the Degree
Master of Science in the
School of Mechanical Engineering

Georgia Institute of Technology
December 2011

AN EXPERIMENTAL STUDY OF ACOUSTICALLY INDUCED

ROCKING MOTION OF SIMPLE ASYMMETRIC GEOMETRIES

Approved by:

Dr. Peter Rogers, Advisor
School of Mechanical Engineering
Georgia Institute of Technology

Dr. Mardi Hastings
School of Mechanical Engineering
Georgia Institute of Technology

Dr. Francois Guillot
School of Mechanical Engineering
Georgia Institute of Technology

Date Approved: November 11, 2011

ACKNOWLEDGEMENTS

TABLE OF CONTENTS

LIST OF TABLES

LIST OF FIGURES

SUMMARY

Otoliths are stone-like structures in the inner ear of fish that play a crucial role in fish hearing. The original object of this research was to determine if any rocking motion was present in an otolith suspended in tissue phantom when subjected to a plane acoustic wave. Measuring the motion of an actual otolith proved to be beyond the limits of project's resources, so an aluminum hemisphere suspended in water was studied instead. The hemisphere was chosen because it was the easiest shape to measure accurately, had the asymmetry necessary to investigate the relevant physics, and had been the subject of some theoretical modeling. A plane standing wave was generated in a short open ended thick-walled cylindrical-waveguide with the waveguide's axis perpendicular to the symmetry axis of the hemisphere. Measurements were taken along the hemisphere from top to bottom to determine if any rocking actually occurred. The expected vertical vibrational motion and symmetry-forbidden horizontal vibrational motion were also measured. The horizontal displacement of the hemisphere at each point was determined by using an ultrasonic vibrometer. The vertical motion was measured using alternative other sensors and methods, such as an accelerometer and Laser Doppler Vibrometer (LDV).

The results from this experiment showed a small amount of rocking, but less than predicted. The vertical motion was around ten times greater in magnitude than the rocking motion at the edge, where it is largest. Additional follow-up experiments were then conducted to determine if any experimental artifacts, such as position in the tank and method of mounting, contributed to the overall result.

Additional testing was then done on a series of semicircular cylinders to determine if their motion matched theoretical predictions. In this case, rocking was also present and was found to be on the order of the motion of the hemispheres. This motion was found to be smaller than published theoretical results.

These results can ultimately be used to predict and understand the motion of more complex geometries, like otoliths.

CHAPTER 1

INTRODUCTION

Motivation

The original goal of this research was to conduct an experimental test of a theoretical model produced by Krysl, et al., on the motion of an otolith in water when subjected to a low-frequency acoustic wave [1]. An otolith is a dense stone-like structure within a fish ear that plays an important role in the directionalization of hearing in fish. When an otolith is excited by a plane acoustic wave, the usual assumption is that the otolith will move back and forth in the same direction as the incident wave propagation. Krysl's model, however, predicted rocking and other transverse motions in addition to motion in the incident wave direction. His model also predicts the same motions in simpler asymmetric geometries, like hemispheres. Since accurately testing the model for an otolith proved to be beyond the limits of resources, the focus moved to testing the model for simpler shapes that had also been modeled by Krysl. Measuring the motion of simpler shapes and comparing to models gives greater insight into the motions of more complex geometries, like otoliths. Determining the motion of simpler geometries also led to an experimental test of a model by Fan, et al. predicting the motion of infinite hemi-cylinders [2].

Theoretical Models

The first theoretical model tested that predicts the motion of otoliths and other asymmetric geometries is given by Krysl, et al. [1]. The model predicts the motion at low frequencies when the object is subjected to harmonic waves in water. This model shows

rocking motion great enough in magnitude to not be negligible when compared to the motion in the same direction as the incident wave. These results are contrary to the notion that an otolith would only move in the direction of the incident wave. The model also gives predictions for the motion of simpler asymmetric geometries, such as hemispheres. The model for the hemisphere shows that for all frequencies, the ratio of the rocking motion to the motion in the incident wave direction is constant at about 13%.

In a paper published in the Journal of the Acoustical Society of America, Zongwei Fan, et al. propose a theoretical model of acoustic radiation torque [2]. Using this model, they predict the motion of an infinite semicircular cylinder (hemi-cylinder) in a plane standing-wave field. For a hemi-cylinder in a plane standing-wave field, they show that the rotational angular velocity of the object is not zero. This small amount of rocking, if present, should be able to be observed. This rocking motion was very similar to the rocking motion predicted for the otolith, so the same experimental setup was suited well to test these predictions. Tests were done on various length hemi-cylinders and compared to these predictions, the results of which are shown in Chapter 5.

CHAPTER 2

INITIAL TESTING

The original goal of this work was to measure the motion of a cod sagittae otolith when subjected to an incident acoustic wave. The otolith was to be suspended in a tissue phantom to eliminate any influence of a mounting system on the results and to mimic the fish tissue surrounding the otolith *in vivo*. An ultrasonic vibrometer would then be used to measure the displacement of the otolith point by point. Since the otolith is a rigid body and therefore does not bend, measuring the displacement at multiple points would provide enough information to indicate the overall amount of rocking and transverse motion of the shape. Initial tests were done by mounting a sphere of known material and size (in this case a 1" diameter glass marble) in a spherical tissue phantom. Two tissue phantom materials were tested for sound speed, ease of molding, ultrasonic attenuation, and density. The chosen tissue phantom had a sound speed of around 1300 m/s, an attenuation of 0.085, and a density of 984 kg/m^3. These values were the closest to the values for water of a sound speed of 1500 m/s, an attenuation of 0.0022, and a density of 1000 kg/m^3. It was molded into a 4.5" diameter sphere with the glass marble directly in the center. A cylinder made of the same tissue phantom and containing a support rod was molded on top of the sphere so it could be suspended in the water. A speaker on the other side of the tank produced an acoustic wave at a single frequency that traveled through the tank, and the subsequent motion of the marble was then measured by means of a NIVMS (noninvasive vibration measurement system) technique. The NIVMS is a measurement system that sends out an ultrasonic signal from a transducer and demodulates the received

ultrasonic signal which has been modulated by a moving reflector. The signal is sent out

from an outer ring of the vibrometer and the reflection is received by an inner disk. This

system works best when the signal can be directly reflected back to the vibrometer and

when the object is in the focal range. The focal distance is 4-5 inches. This system can be

used to accurately measure displacements on the order of 10^{-8} m with a spatial resolution

of the beam of about 1mm [3]. There is uncertainty in the measurements based on the

noise level. A diagram of the setup is shown in Figure 1.
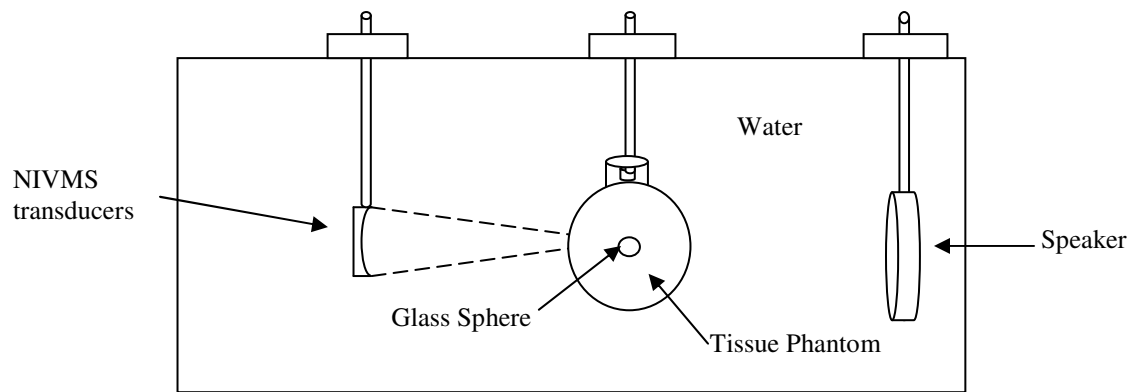
Figure 1. Initial Test Setup

Since the theoretical motion of a simple shape like a sphere could be calculated,

the results from this test could be compared with theory to validate the setup. Then, the

marble could be replaced with an otolith and the testing of the otolith could begin. Even

with this simpler control test, though, there were complications. First, it was difficult to

get the transducer signal to pass straight through the curved tissue phantom surface and

return again. Also, since the marble itself was curved, the transducer signal was reflected

at an angle off of it as well. The test was also done in a small tank, so the acoustic wave

from the speaker was reflected off all the walls of the tank, which created a complicated,

non-uniform field. Even with the addition of an acoustically absorptive material on the

tank walls, the tank was too small to contain a uniform field. Therefore, the resulting motion of the marble was not what was predicted by theory.

A potential solution to this problem was to conduct further experimentation 6' underwater in a large 25' deep tank. This would solve the problem of a non-uniform field caused by the small tank, but it introduced additional problems. First, suspending the assembly underwater was a challenge, as was accurately adjusting the height of the NIVMS to perform the scans. Without being able to see and adjust the assembly, this option was discarded.

There were additional complications in moving to the otolith testing in addition to the problems already observed from the sphere test. For one, the otolith was so small that it would be difficult to measure multiple points along the length with enough accuracy to determine the overall motion of the object. Measuring multiple points was also an issue because the otolith was not symmetric in any direction. Since the otolith was not a flat surface, the incident transducer signal would be reflected off at an angle that would change with position along the otolith, so the signal measured by the NIVMS would not necessarily be representative of the actual motion of that point.

Simplification of Experiment to Hemisphere

After taking into account all of these factors, it was decided to measure the motion of a simpler shape suspended in water. Since it was determined that an object would still behave in much the same the same way in water as in a tissue phantom, it would be much simpler to conduct experiments in water. This way, the results would be better characterized, since all the water parameters are well known. Determining how simpler shapes behave when excited by an incident acoustic wave is valuable since these

objects are easier to characterize and model, yet exhibit the same features as more complicated objects like otoliths. The objective would thus be to examine the simplest system which might be expected to exhibit a rocking motion when excited by an acoustic plane wave.

A 1" diameter aluminum hemisphere was chosen as the first test object for several reasons. First, the hemisphere was not symmetric. Such asymmetry was present in the otolith as well and is likely required for rocking to occur. Also, Krysl's model predicted significant rocking for a hemisphere. Translational motion in both the vertical and horizontal directions (as shown in Figure 2) could also be easily observed.
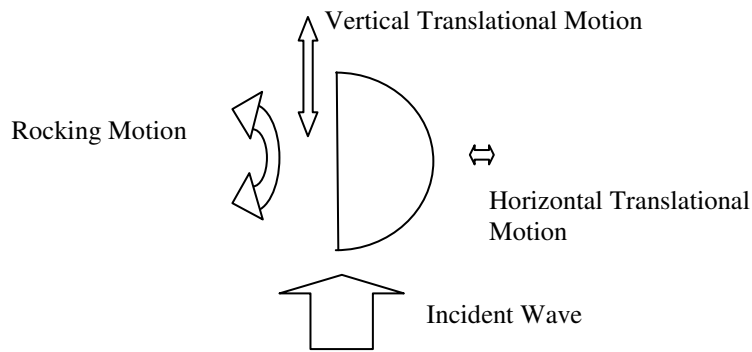
Figure 2. Possible Motions of Hemisphere

The larger size of the hemisphere made it possible to accurately measure more than a dozen evenly spaced points from the top to bottom while the object still meeting the "acoustically small" condition. Aluminum has a density similar to that of an otolith (both about 2.7 g/cm^3), and is sufficiently rigid to be able to neglect elasticity. The flat side of the hemisphere also provided a much better reflecting surface for the NIVMS than an otolith would. To make sure the mounting of the hemisphere did not affect its motion, the supports were attached along the same plane as the center of mass. This would assure that any torques generated by the acoustic field about the center of mass would be the same as

6

if the object was suspended in the absence of gravity. The tests were done in a thick-walled stainless steel cylindrical tank that served as a waveguide which assured that only plane waves would be present in the chamber at the frequencies of interest. Thus, the problem of a non-uniform field in the tank was also addressed.

CHAPTER 3

EXPERIMENTAL SETUP

The sections below show the details of all parts of the hemisphere experiment.

Tank Setup

The hemisphere was suspended in an open-top rigid steel cylinder filled with water. The cylinder was 14" deep and had an inside diameter of 10" with 1.5" thick walls on all sides. A piston-shaker assembly that created a plane wave that traveled vertically through the tank was mounted to the bottom. This tank was chosen because it was rigid and acted as a waveguide so only plane waves would be present. It was also radially symmetric, so the tank itself would have no effect on the results. The NIVMS transducer was also suspended with its symmetry axis oriented horizontally in the water and pointed at the flat side of the hemisphere to measure its horizontal transverse motion. A rod holding the transducer was attached to a positioning system which allowed precise control over the location of the transducer. This allowed vertical scans of horizontal motion of the hemisphere to be made along the central axis. A diagram of the assembly is shown below in Figure 3.
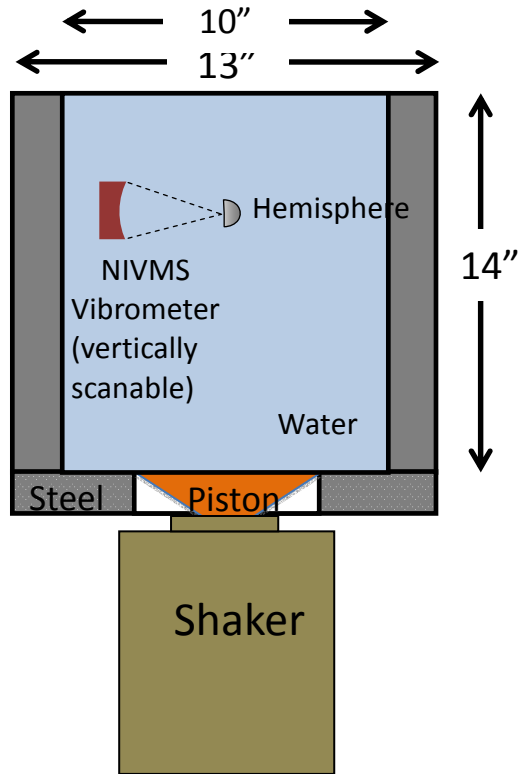
Figure 3. Cylinder Assembly

The shaker was controlled by a computer through a LabView program. A pure sinusoidal wave at a specified frequency and amplitude was sent to the shaker for each test.

Hemisphere Mounting

To suspend the hemisphere in the tank, two pieces of nylon fishing line were glued to the top of the hemisphere at two attachment points such that the attachment points lay in the same vertical plane as the center of mass. The other ends of the line were then attached to a cylindrical metal frame that was sitting on the bottom of the tank. The annular bottom of the frame was around the shaker but did not touch it. A picture of the line attached to the hemisphere is shown in Figure 4 and a picture of the metal frame with the hemisphere suspended is shown in Figure 5.

Figure 4. Hemisphere Attachments

Figure 5. Hemisphere Mounting

Sensors

A hydrophone was also placed at the bottom of the tank. From the pressure

measurements, the motion of the water in the chamber could be determined. The position

and alignment of the hemisphere and measurement devices in the tank is shown in Figure 6 and Figure 7. The yellow structure is a residual from another application and plays no role in this experiment other than providing support.

Different types of sensors were used to determine the vertical motion of the hemisphere. The hydrophone mentioned above, as well as an accelerometer and a Laser Doppler Vibrometer (LDV) were used. Determination of the vertical motion will be discussed in depth in Chapter 4.
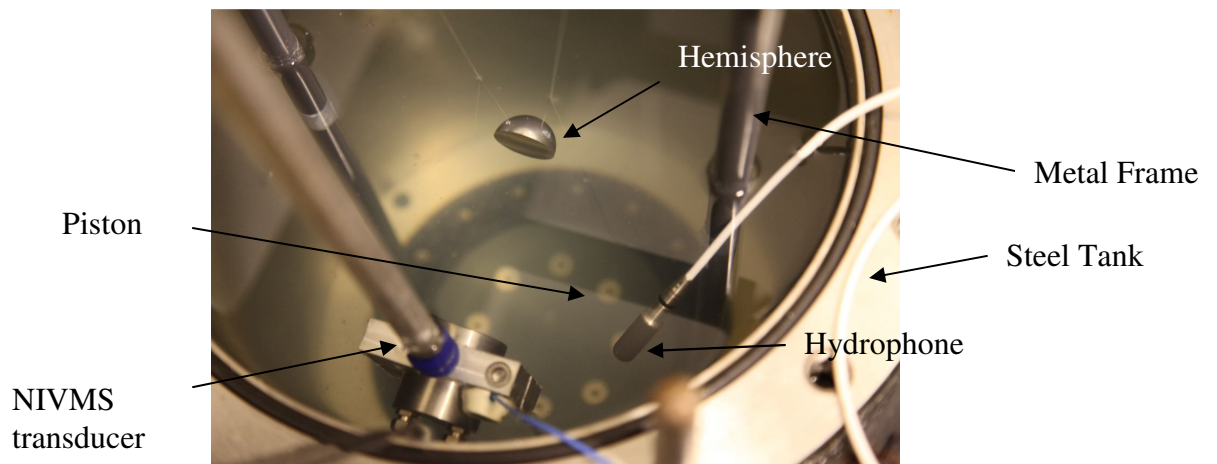
Figure 6. NIVMS Transducer, Hemisphere, and Hydrophone in Tank

Positioner
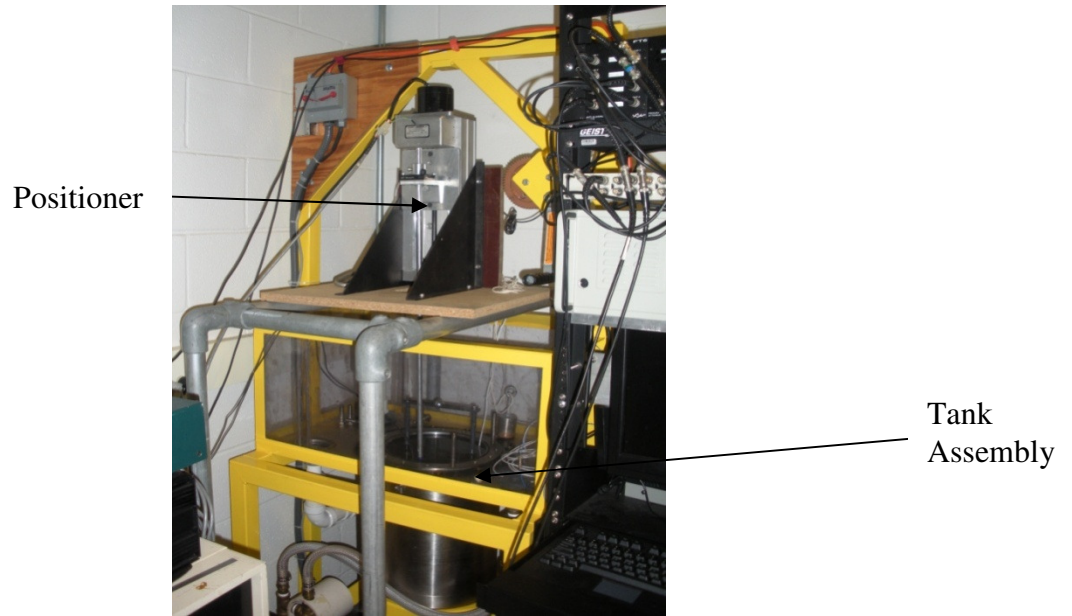
Tank
Assembly

Figure 7. Overall Assembly

Tank Response

Ideally, the pressure in the tank should be radially uniform and the vertical

pressure gradient should be uniform. Tests were done with the hydrophone to determine

the pressure gradient from the bottom to the top of the tank and the change in pressure at

the bottom of the tank as a function of frequency and shaker drive level. Figure 8 shows

the pressure gradient along a vertical line through the center of the tank at various

frequencies. The distance between each point number on the x-axis is one inch.
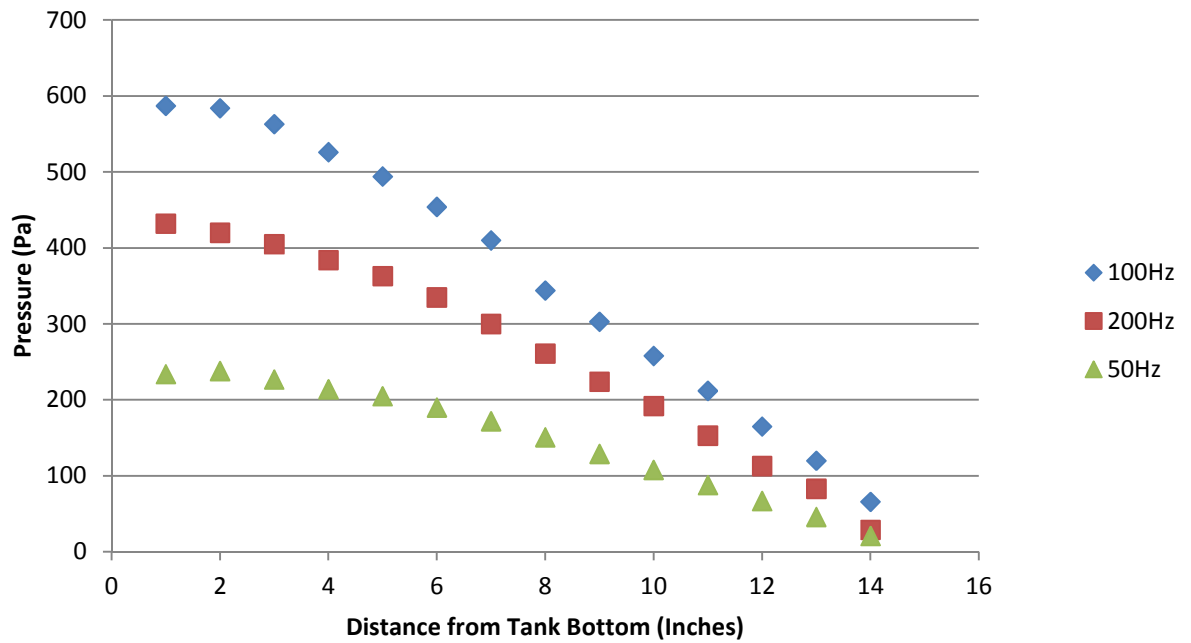
Figure 8. Hydrophone Gradient

From this figure, it is obvious that the pressure along the measurement line was not completely uniform. This is due to the effect of the size of the piston which is smaller than the diameter of the cylinder. The radial uniformity of the field is imperfect near the piston due to evanescent modes. Obviously, the middle of the bottom of the tank was not a desirable location to measure the pressure. Figure 9 shows the pressure measured by the hydrophone as a function of frequency at multiple drive levels and Figure 10 shows the pressure as a function of shaker drive level at multiple frequencies, all measured near the bottom of the tank as far from the piston as possible.
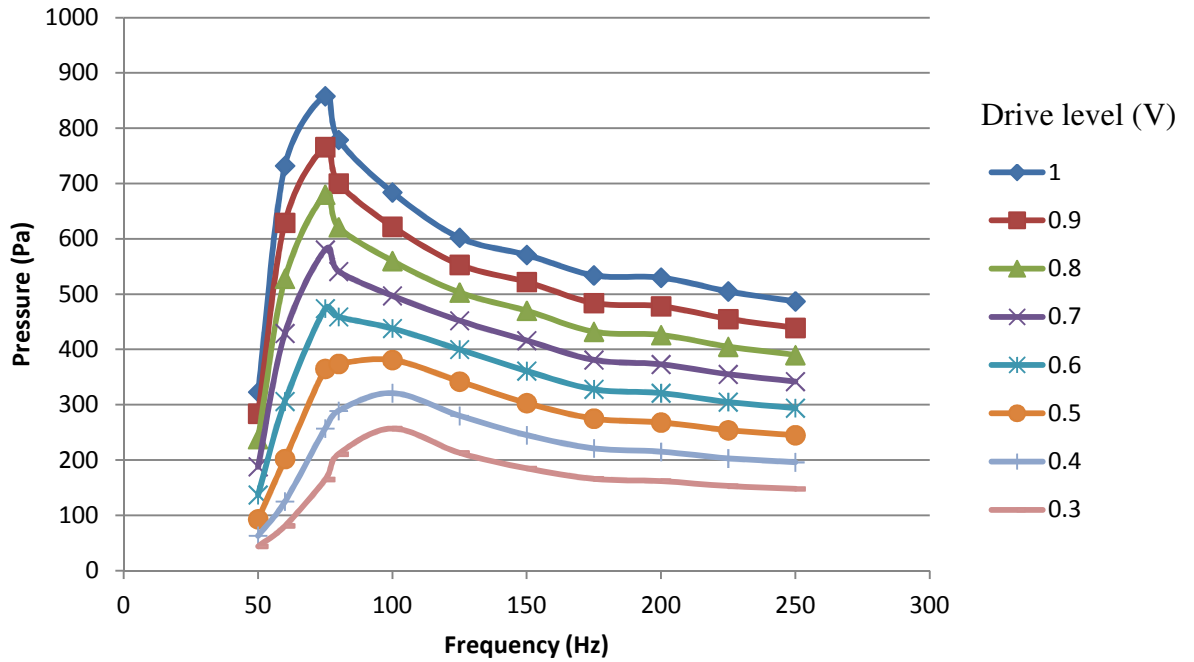
Figure 9. Pressure as a Function of Frequency at Eight Drive Levels

At each drive level, there is an apparent resonance around 70Hz. This could have been caused by a resonance in the piston transducer or in the tank. Because of this phenomenon, data was only taken at 100Hz and 200Hz, in a region where the pressure change with frequency was more predictable. Measurements at these two frequencies can also be compared with the predictions of the model at the same frequencies.
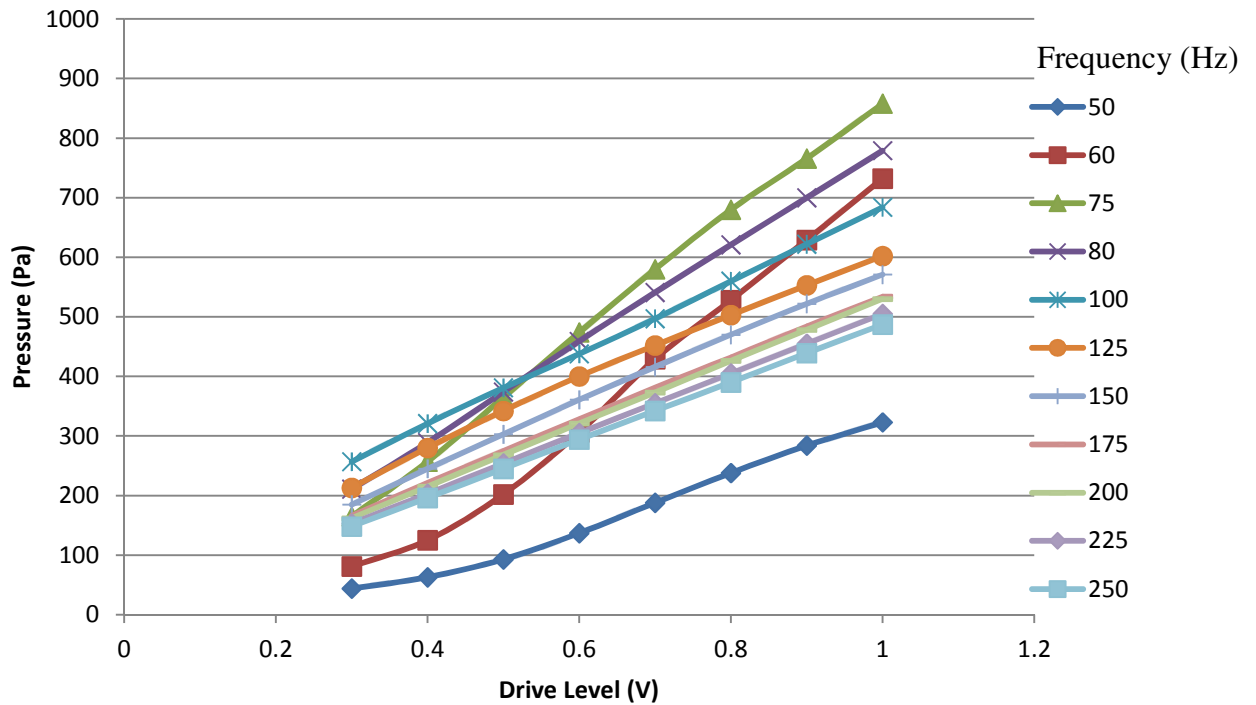
Figure 10. Pressure as a Function of Shaker Drive Level at Multiple Frequencies

A linear increase in drive level produced a linear increase in pressure at all frequencies. The slope of the line was greater for the frequencies close to the resonance of the tank, but was very similar at all other frequencies measured.

Ultrasonic Vibrometer

The NIVMS vibrometer transducer consists of an outer transducer ring surrounding the center disk which was the ultrasonic source, and a center disk which received the signal reflected by the hemisphere. The transducer was placed so that the flat side of the hemisphere was at the focal length of the transducer. The NIVMS system determines vibrational motion in the direction of the transducer axis by demodulating the received ultrasonic signal which has been modulated by the moving reflector [3]. First, a waveform generator was used to send out a pulse signal that was synchronized with a 10 MHz clock. That signal then went through a bandpass filter that allowed frequencies

15

between 0.07 and 3.5 MHz to pass and an attenuator before being amplified and sent to the transducer. The signal received by the transducer went through a differential amplifier before it was recorded by the A to D card in the computer. A diagram of the NIVMS system is shown below in Figure 11.
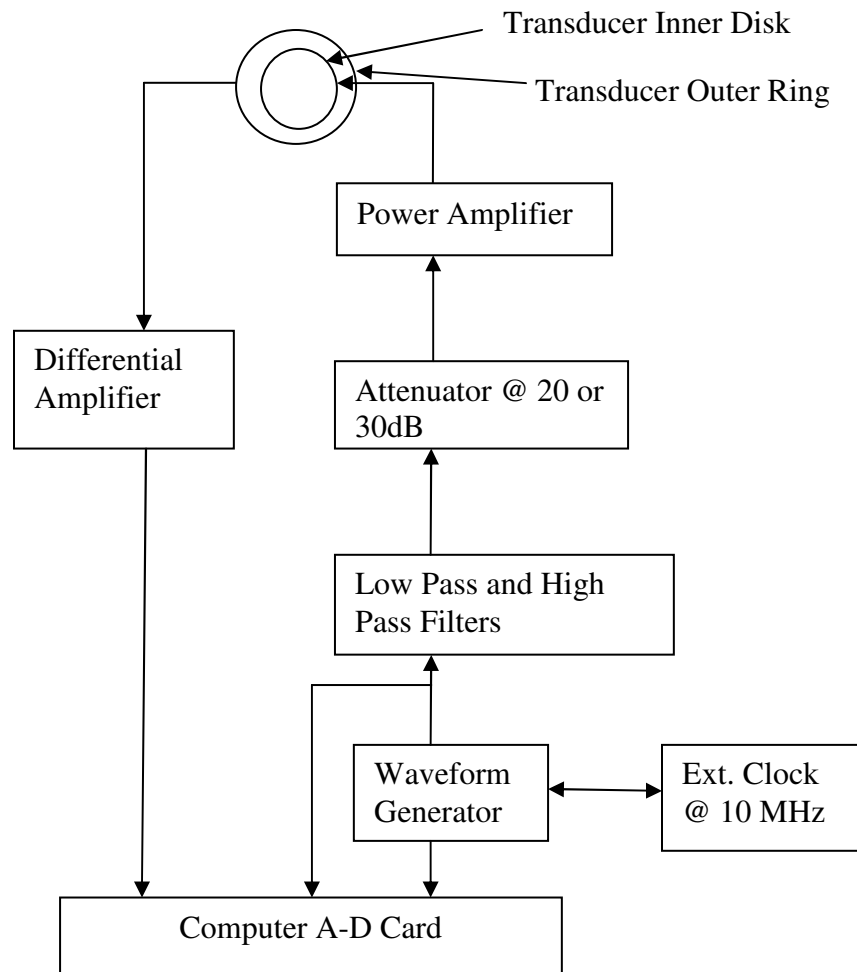
Figure 11. Diagram of NIVMS Setup

The signal sent through the waveform generator consisted of a single pulse with frequencies ranging from 1.5-3.2 MHz. The duration of the signal was 5000 points, which corresponded to 0.5 ms. The pulse repetition rate was 2000 cycles per second.

Figure 12 shows a close up of the signal in the time domain, and Figure 13 shows the same signal in the frequency domain.
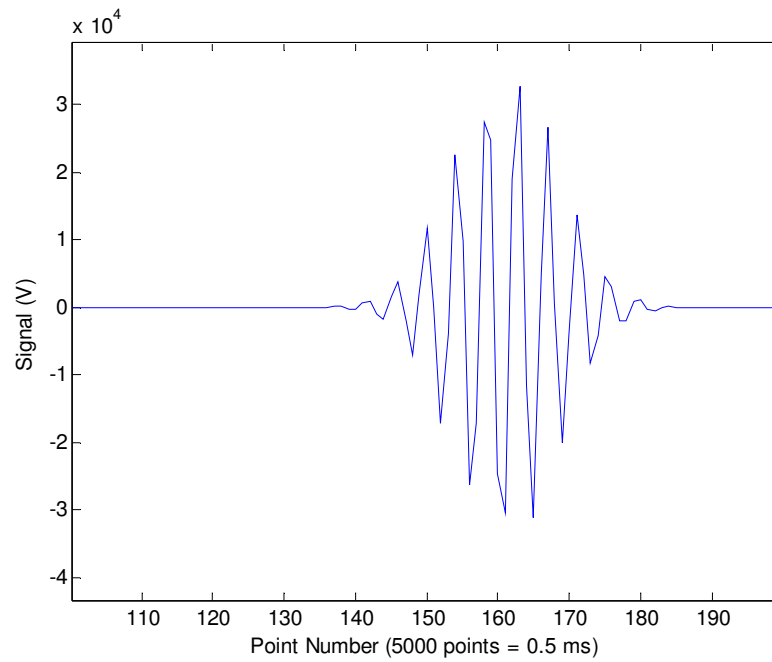
Figure 12. Transducer Signal in Time Domain
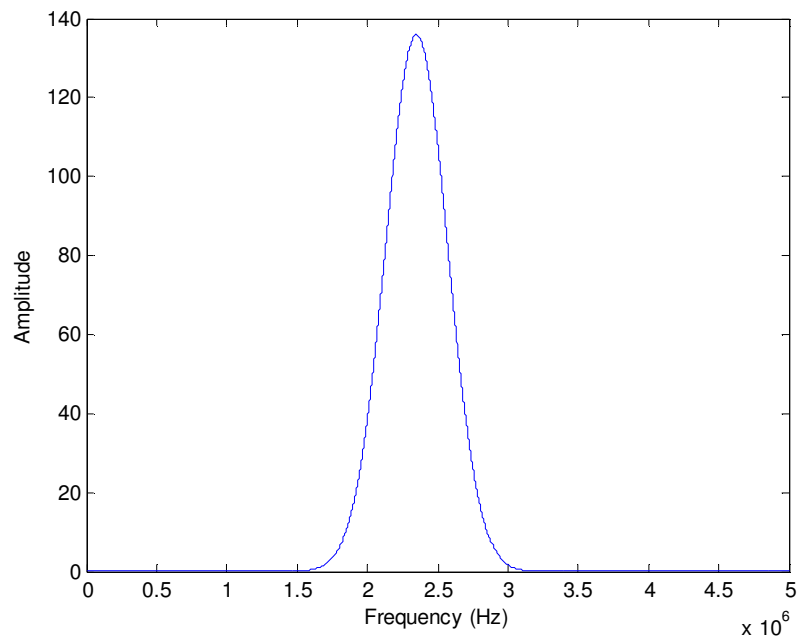
Figure 13. Transducer Signal in Frequency Domain

For each test, data was collected for 20 half second periods and averaged to increase the signal-to-noise ratio. This data was then run through a code designed to demodulate the received transducer signal to extract the displacement of the reflector in the direction of the transducer axis. The demodulation scheme and entire setup is explained in great detail by Martin [3]. An example of a single reflected signal is shown in Figure 14 below. The large spike between points 1000 and 1500 represents the hemisphere.
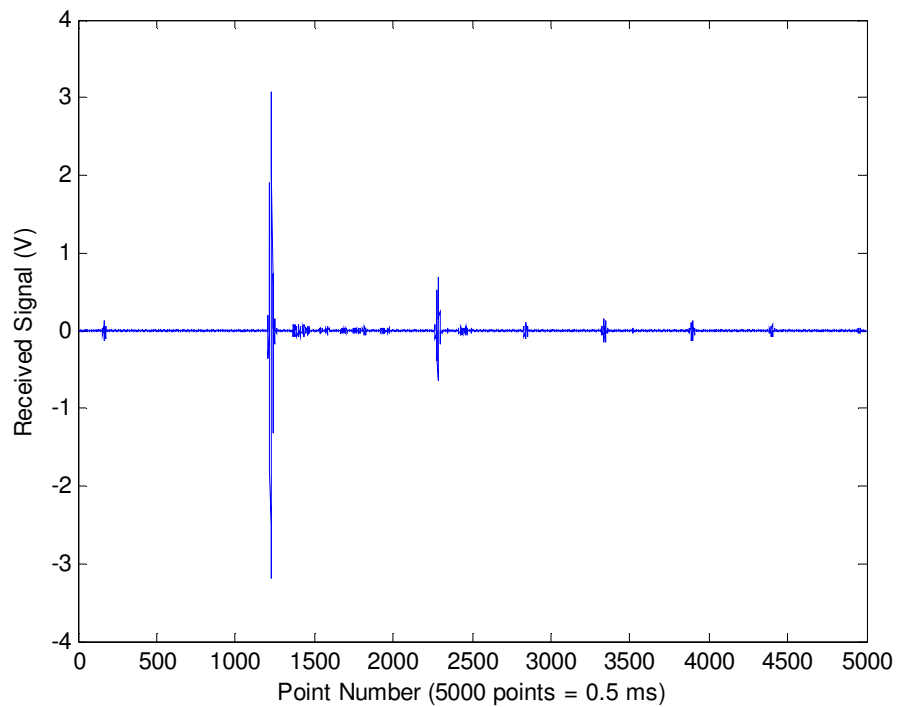
Figure 14. Reflected Signal

CHAPTER 4

HEMISPHERE TESTS

Displacement Measurements at 100Hz and 200Hz

The positioner was used to get a scan of the displacement of the hemisphere from top to bottom along the centerline of the flat surface. The locations of the top and bottom of the hemisphere were determined by monitoring the transducer signal on an oscilloscope and identifying the top and bottom by where the reflected signal disappeared. The range was divided into 15 equal segments over the 1" diameter of the hemisphere. The positioner was then used to move the transducer to each segment, where 20 trials of 0.5 seconds each were taken and averaged to increase the signal to noise ratio. The transducer, the shaker, and the waveform generator were all synchronized to the same 10MHz clock reference. To increase the accuracy of the results, four scans were done (from top to bottom) at each frequency (100Hz and 200Hz).

Since the NIVMS transducer assembly was in the same tank as the hemisphere and was subjected to the same acoustic excitation, the motion of the assembly needed to be taken into account. After all the data was collected from the hemisphere, it was removed from the tank and replaced by a large steel cylinder oriented with its axis vertical. The cylinder was large and heavy enough to be considered motionless in the horizontal direction, so it could be used as a stationary reference to measure the motion of the NIVMS transducer assembly. The same scans were done at the same locations as before, and the results were later subtracted from the hemisphere data to get the motion of just the hemisphere alone.

The raw data was then numerically converted into the corresponding displacement of the hemisphere at each point. By plotting the magnitude of the displacement at each point along the scan, the overall motion of the hemisphere could be observed. Figure 15 and Figure 16 show the motion at each frequency, averaged over all trials. On each figure, the x-axis represents the point number along the hemisphere from top to bottom, with the distance between each point being approximately 1/15". The y-axis is the measured horizontal displacement of the flat side of the hemisphere. The error bars on this and every figure represent the standard deviation of the data at each point.
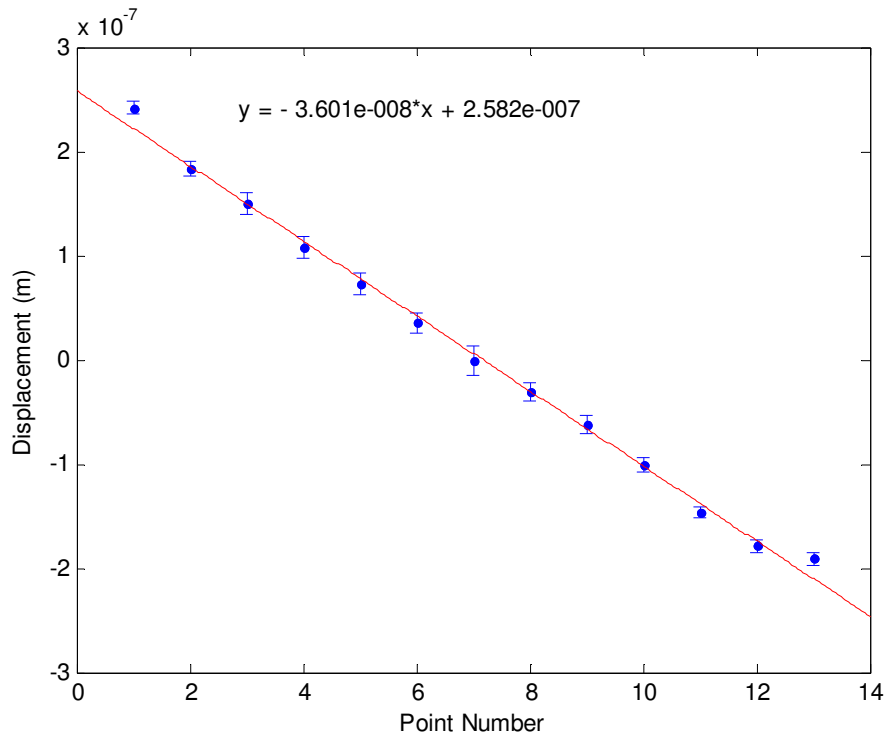
Figure 15. Hemisphere Motion at 100Hz
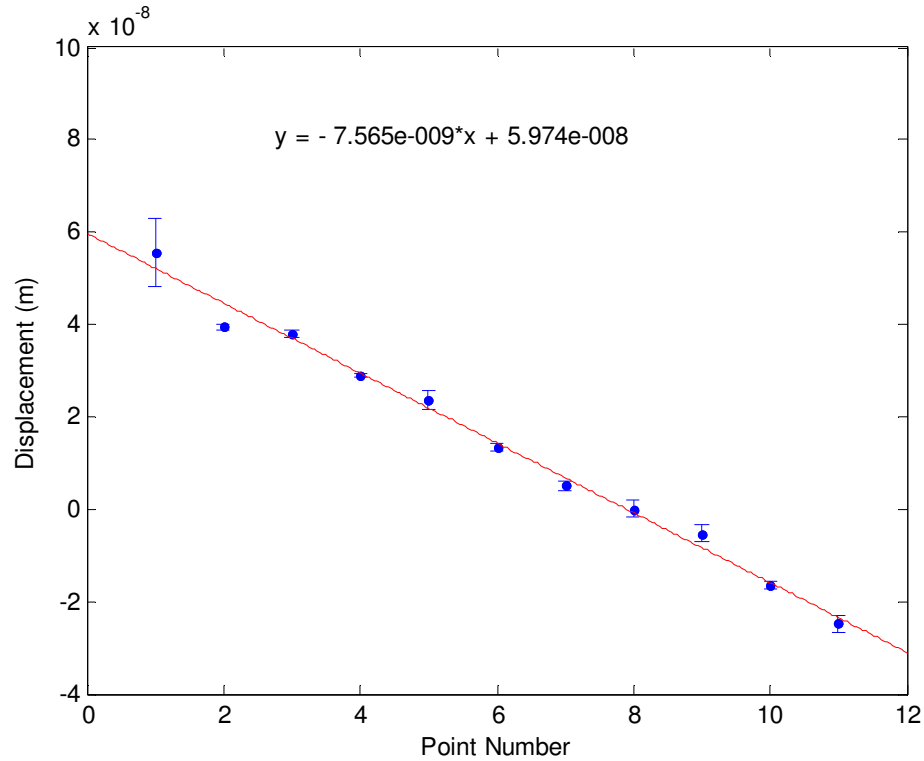
Figure 16. Hemisphere Motion at 200Hz

The motion shown in each of these figures is a combination of rocking about the center of mass and horizontal translational motion (horizontal displacement of the center of mass of the hemisphere) which is considerably smaller. From the linear curve fit shown on the figures, the maximum displacement and transverse motion can be inferred. The maximum rocking displacement is found by measuring the difference of the displacement of the center of the hemisphere and the displacement of the end, and the transverse motion is the amount of displacement at the center point. These values at each frequency are summarized in Table 1.

Table 1. Motion of Hemisphere at 100Hz and 200Hz

	100Hz	200Hz
Maximum Rocking Displacement	2.6e-7	6e-8
Transverse Displacement	5.4e-9	1.9e-8

Discussion

The results show the hemisphere acting like a rigid body, as expected. The rocking and the transverse motion are both rigid body motions, and no deformation of the hemisphere is observed. Also, the maximum rocking displacement of the hemisphere at 200Hz is significantly smaller than the corresponding motion at 100Hz. This is also to be expected, since the force acting on the body at 200Hz results in a smaller displacement. The transverse motion in each case is also much smaller than the rocking motion.

Vertical Motion

To fully understand the meaning of these results, they need to be compared to the vertical motion of the hemisphere under the same conditions. This proved to be more difficult than one might imagine, since the NIVMS could not be used for this purpose. Three different methods were used to determine the vertical motion of the hemisphere accurately. This allowed for greater confidence in the results if multiple methods produced similar results. One method utilized a Laser Doppler Vibrometer (LDV) to measure the velocity of the top surface of the hemisphere and then convert to displacement. The second approach was to attach a neutrally-buoyant accelerometer to the hemisphere and then convert the measured acceleration to displacement. The last

method was to use a hydrophone to measure the pressure at the bottom of tank, use that information to calculate the velocity of the water, and use a model to infer the associated motion of the hemisphere. The results of each of the three methods are shown below. The displacement of the water surface was then tested with the same three methods as another test of the three sensors' accuracy.

Laser Doppler Vibrometer (LDV)

The first way of measuring the vertical motion was with an LDV (Polytec PDV-100). Since the laser was passing through both air and water, several additional factors had to be considered. First, a corrective factor of 1.33 was included in the conversion to account for the difference in the optical indexes of refraction between the two media. Second, since the surface of the water was moving and would have affected the reading on the LDV, a cylindrical glass window was partially submerged on the surface of the water directly above the hemisphere. This setup is shown in Figure 17.
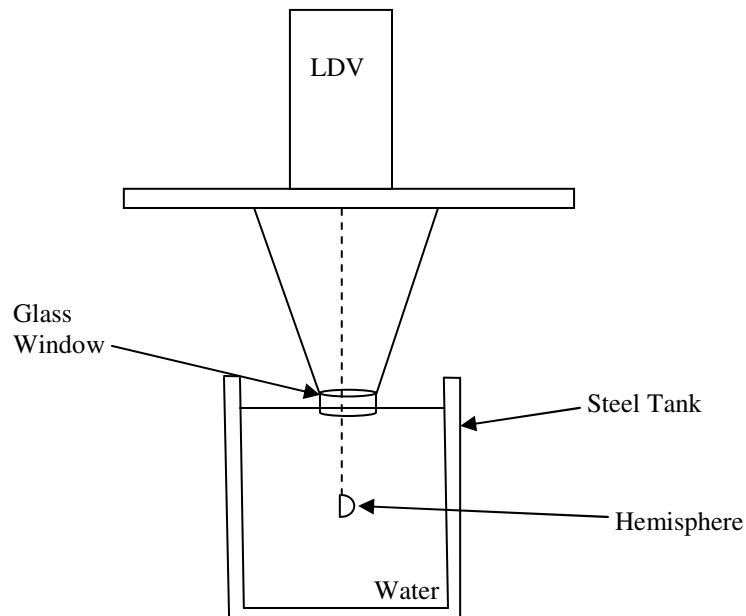
Figure 17. Setup for Vertical Motion with LDV

Since the glass window was essentially fixed in place, the laser beam passing through it was not exposed to the motion of the water surface. The LDV was placed so the laser was focused on the top of the hemisphere and the measurements were recorded. Since the LDV produced measurements of velocity in volts, the conversion in Equation 1 was used to obtain displacement in meters.

$$d = \frac{reading\ in\ V * \frac{calibration\ factor}{1000}}{2\pi f} / 1.33 \qquad \text{(Equation 1)}$$

In this formula, d is the vertical displacement and f is the frequency. The calibration factor was 5 mm/s/V and the factor of 1000 comes from the conversion of mm/s to m/s. The 1.33 accounts for the change in index of refraction and the denominator comes from integrating the velocity to get displacement.

Multiple readings for each frequency were taken and averaged. After doing the conversion, the results were a vertical displacement of 3.39 x 10^{-6} m at 100Hz and 6.30 x 10^{-7} m at 200Hz.

Hydrophone

The hydrophone measurements were initially taken at the bottom of the tank since that was the easiest way to ensure all measurements were taken at the same depth. The hydrophone used had a calibration constant of 31.6µV/Pa and a gain of 10. With the pressure at the bottom, the depth of the tank, and the assumption that the pressure changed linearly with depth, the pressure gradient could be found. However, after measuring the pressure as a function of depth in the tank (see Figure 8), it was found that the gradient was not completely linear at the bottom of the tank. Therefore, the pressure and depth were taken at the middle of the tank to allow for a linear gradient to still be

used. Equation 2 shows how the pressure gradient was used to determine the motion of the water in the tank.

$$\rho_o \omega^2 \xi = -\nabla p$$ (Equation 2)

In this formula, ρ_o is the density of water, ω is the frequency, ξ is the displacement of the water, and ∇p is the gradient of the pressure. The displacement of the water was then used in Equation 3 to determine the motion of the hemisphere, where d is the displacement of the hemisphere, and ρ_h is the density of the hemisphere.

$$d = \xi \frac{3}{\frac{2\rho_h}{\rho_0}+1}$$ (Equation 3)

The pressure measurements at a depth of 7" were 344Pa RMS at 100Hz and 261Pa RMS at 200Hz. From these measurements, the vertical motion of the hemisphere at 100Hz was calculated to be 3.17 x 10^{-6} m and the vertical motion at 200Hz was 6.00 x 10^{-7} m.

Accelerometer

As another check on the validity of the vertical motion measurements, an accelerometer attached to the hemisphere was used. The accelerometer was had a gain of 10 and a calibration constant of 114 mV/g. It was neutrally buoyant, so its mass should not affect the measurements. The calibration constant was checked by doing an additional test of placing the accelerometer on the surface of the water and focusing the LDV on the accelerometer. By comparing the numbers from each device, the calibration constant was accurately determined. The accelerometer was then attached to the bottom of the hemisphere, and its output was converted to displacement in meters using Equation 4.

$$d = \frac{\frac{reading\ in\ mV}{gain} * \frac{9.8}{calibration}}{(2\pi*f)^2}$$ (Equation 4)

In this formula, f is the frequency, and d is the vertical displacement, as before. The

numerator of the equation converts the reading from mV to m/s^2, and the denominator is

the result of integrating the acceleration twice to obtain displacement.

As with the LDV measurements, multiple readings were taken and averaged. The

results from these calculations are a vertical motion of 3.45 x 10^{-6} m at 100Hz and 6.01 x

10^{-7} m at 200Hz. The results of the three different ways of finding vertical displacement

are summarized in Table 2 below.

Table 2. Comparison of Three Methods of Finding Vertical Displacement Amplitude

	100Hz	200Hz
LDV	3.39e-6	6.30e-7
Hydrophone	3.17e-6	6.00e-7
Accelerometer	3.45e-6	6.01e-7

Motion of Water

As a further check on the results, the motion of the water was measured with each

of the three sensors. The motion of the water was already calculated from the hydrophone

data (ξ in Equation 3), so new measurements were only taken with the accelerometer and

the LDV. The accelerometer was floated on the surface of the water and the

measurements were converted to displacements using the same formula. For the LDV,

there was an additional challenge. Since the laser would pass straight through the surface

of the water, a reflective surface had to be placed on the surface without disrupting the

motion of the water. Without such a surface, the measurements taken with the LDV

would have been a combination of the motion of the surface and the motion of the piston

at the bottom of the tank. A thin sheet of plastic was coated with black ink and placed on the surface provided the needed reflective surface. The results from each of these tests are shown in Table 3 below.

Table 3. Comparison of Three Methods of Finding Motion of the Water Surface

	100Hz	200Hz
LDV	6.64e-6	1.31e-6
Hydrophone	6.93e-6	1.32e-6
Accelerometer	6.93e-6	1.30e-6

Comparison and Discussion

At both frequencies, the motion of the water was about twice that of the hemisphere. Comparisons can be made between the vertical and transverse motions of the hemisphere. The average vertical motion (found by averaging the results of all three methods) was 3.33×10^{-6} m at 100Hz and 6.13×10^{-7} m at 200Hz, and the maximum rocking motion was 2.5×10^{-7} m at 100Hz and 6×10^{-8} m at 200Hz. In other words, at 100Hz, the vertical motion was 13.3 times larger than the rocking motion, and at 200Hz, the vertical motion was 10.2 times larger than the rocking motion. In both cases, the rocking motion is significantly smaller than the corresponding vertical motion. Krysl's model shows no change in the ratio of vertical to rocking motion, while this data does show a difference.

Validity of Data

Transducer Drive Level

After gathering the results from the previous tests at 100Hz and 200Hz, it was necessary to show that the results were not influenced by the means of data collection. To do this, parameters that should not have influenced the data were changed to see if the overall result changed. One parameter that could have been affecting the data was the radiation pressure from the NIVMS transducer. The thought was that the radiation pressure could cause the flat surface of the hemisphere to tilt with respect to the vertical plane proportionally to the radial offset of the ultrasonic beam. The hemisphere would then appear to be rocking. To make sure that the radiation pressure was not causing any of the horizontal motion that was observed in the data, a new test was performed. In this test, three different transducer drive levels were used to determine if lowering the drive level also lowered the maximum measured rocking displacement of the hemisphere. The original tests were done at a 50mV drive level, so that level was used again, as well as 25mV and 16mV. A comparison of the data at these three levels showed no significant change in displacement from one level to the next. Therefore, it was concluded that the radiation pressure from the transducer signal did not affect the results. The only change in data was a slight decrease in the signal to noise ratio at the lower drive level. Figure 18 shows the results at all three levels. In this figure, the x-axis shows the point along the vertical scan of the hemisphere, as with the original data. The y-axis is the displacement in meters at each point.
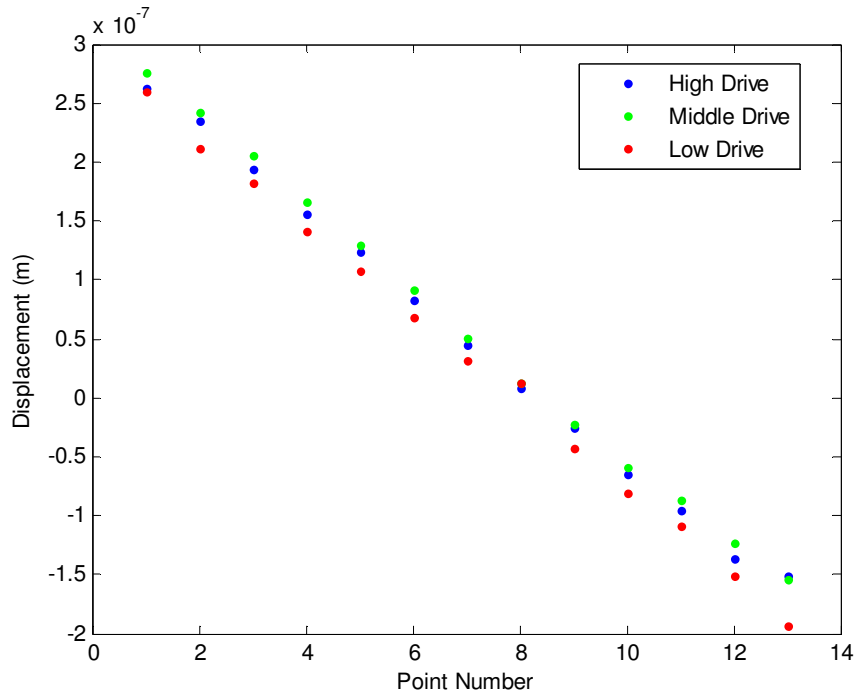
Figure 18. Comparison of Three NIVMS Drive Levels at 100Hz

Hemisphere Mounting

Another factor that could have been affecting the data was the way the hemisphere was mounted. This factor is also most likely the largest source of uncertainty in the data. As shown in the setup, the apparatus supporting the suspended hemisphere was in the tank surrounding the shaker. Any motion of this assembly could have been transferred through the suspension and into the hemisphere, causing extra hemisphere motion. To determine if this was the case, the hemisphere suspension was replaced by a metal frame running above the top of the cylinder assembly without touching it. This arrangement would greatly reduce any motion of the suspension caused by the shaker. A diagram of this setup is shown in Figure 19.

29
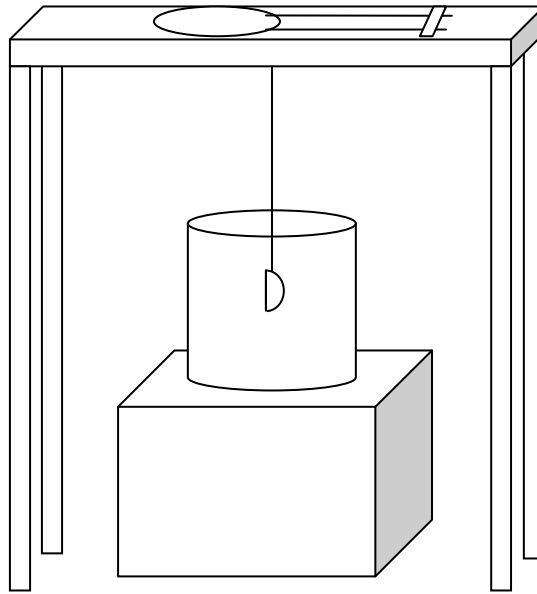
Figure 19. New Hemisphere Mounting Assembly

It was important for these components to be mounted on a separate assembly from the

cylinder so that the motion of the shaker could not transfer to the transducer or

hemisphere and affect the measured motion. The hemisphere was at the same height as

before. Data was then retaken at the same two frequencies (100Hz and 200Hz), and

compared with the data from the previous mounting. The results are shown in Figure 20

and Figure 21.

y = 3.784e-008*x - 3.912e-007
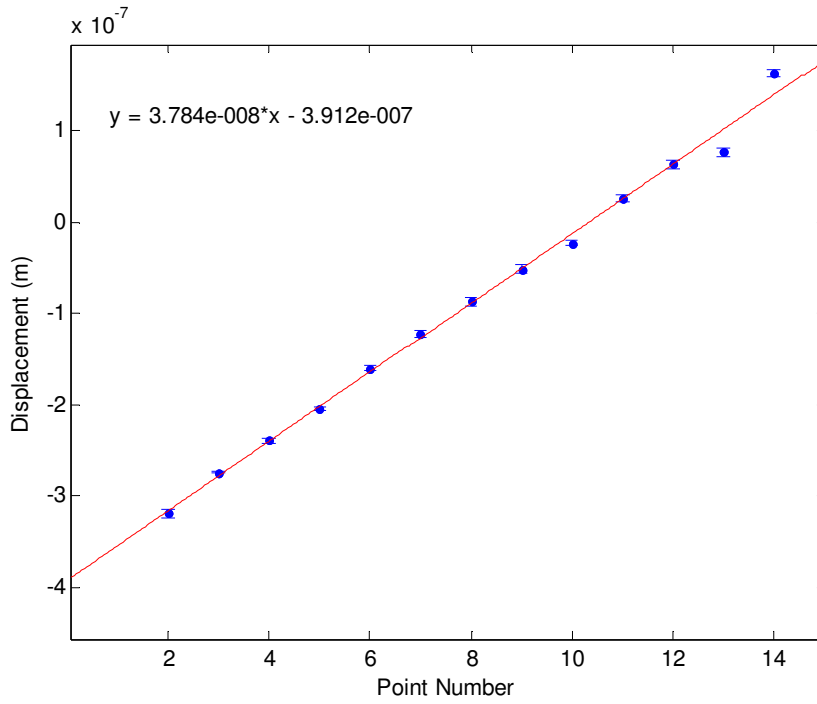
Figure 20. New Mounting at 100Hz

y = 8.837e-009*x + 6.171e-008
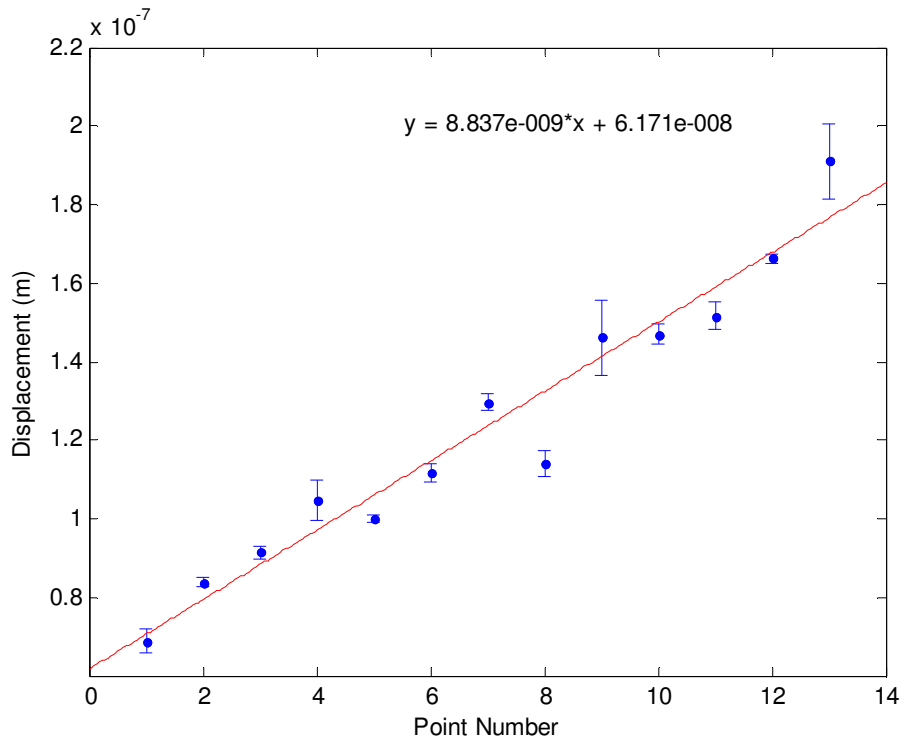
Figure 21. New Mounting at 200Hz

At 100Hz, the data taken with the new mounting is very consistent. The figure shows slightly less overall motion than the data of the previous mounting, but otherwise it is similar. At 200Hz, however, the data was much less consistent and showed much higher displacements. In later tests with the same mounting this pattern is not seen, so some anomaly must have been influencing the results at this frequency. From the results at 100Hz and the physics of the problem, it was determined that keeping the hemisphere mounting assembly outside of the tank would be best.

Hemisphere Position in Tank and Linearity

After doing these two additional tests, one more test was done. The final change was to mount the hemisphere in the center of the tank (7" below the surface) instead of 4" below the surface. This configuration gave the hemisphere less interaction with the surface while still placing it far enough away from the shaker for it to be exposed to only plane waves. Data was taken at 100Hz and 200Hz again with runs at three different shaker drive levels. The shaker was also excited at 0.8V (as before), 0.6V, and 0.4V to test that a linear decrease in drive level corresponded to a linear decrease in hemisphere displacement. Figure 22-Figure 27 show the data at each drive level.
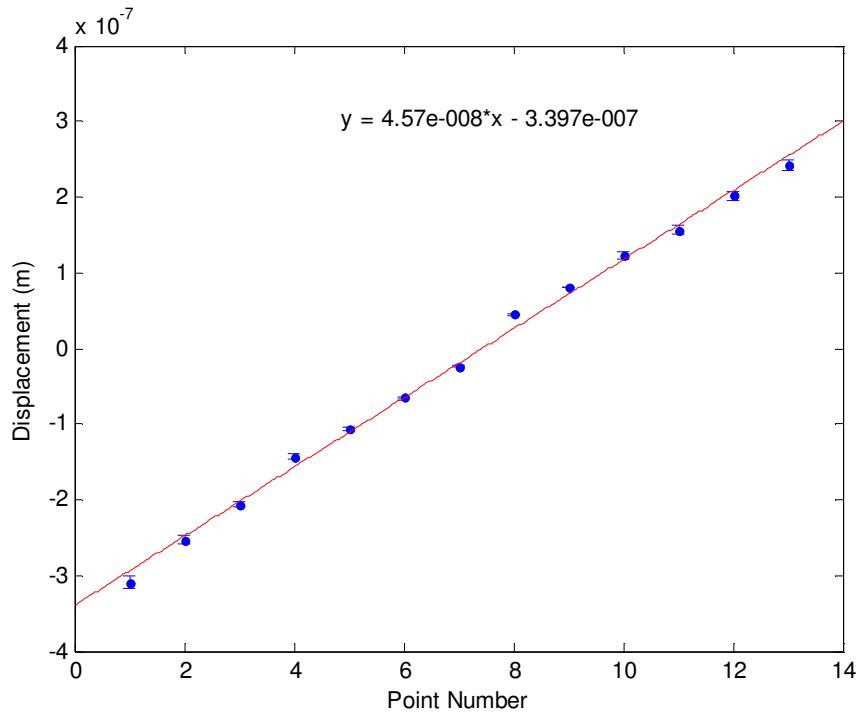
Figure 22. 100Hz Displacement at 0.8V
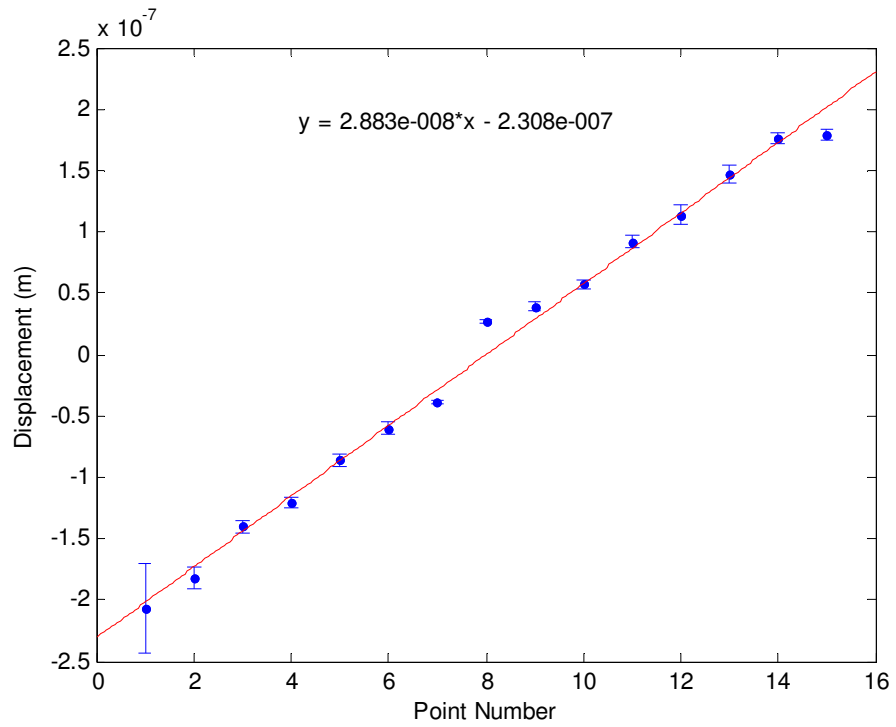
Figure 23. 100Hz Displacement at 0.6V
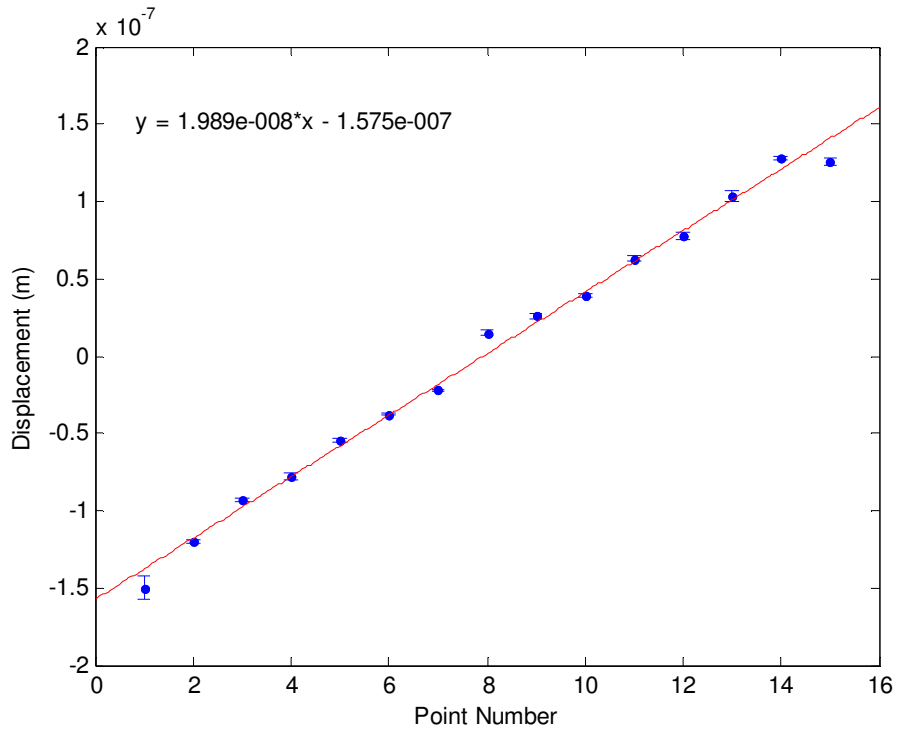
Figure 24. 100Hz Displacement at 0.4V
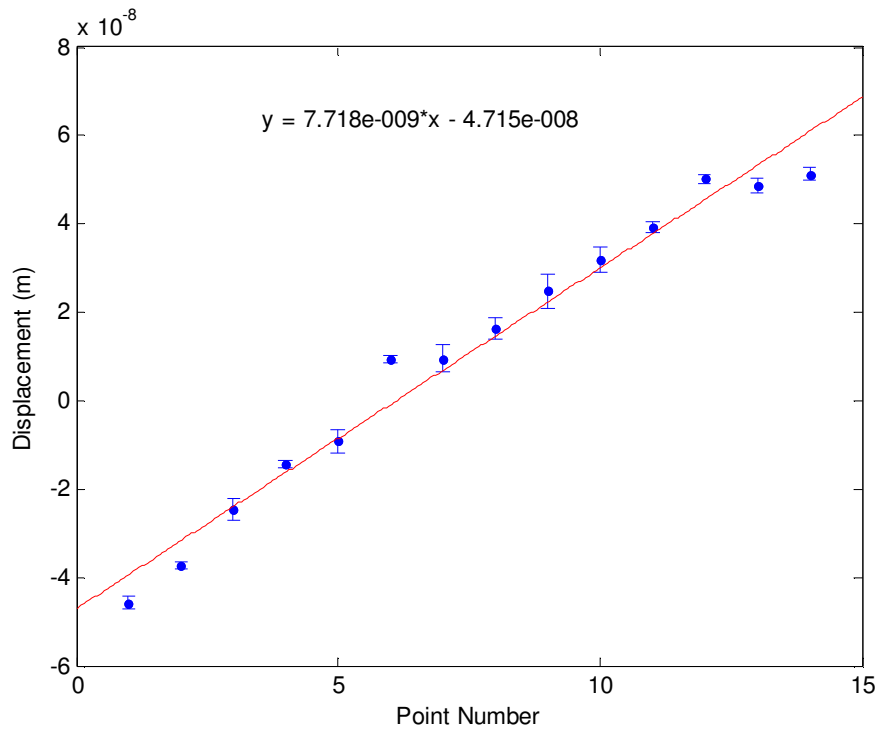
Figure 25. 200Hz Displacement at 0.8V
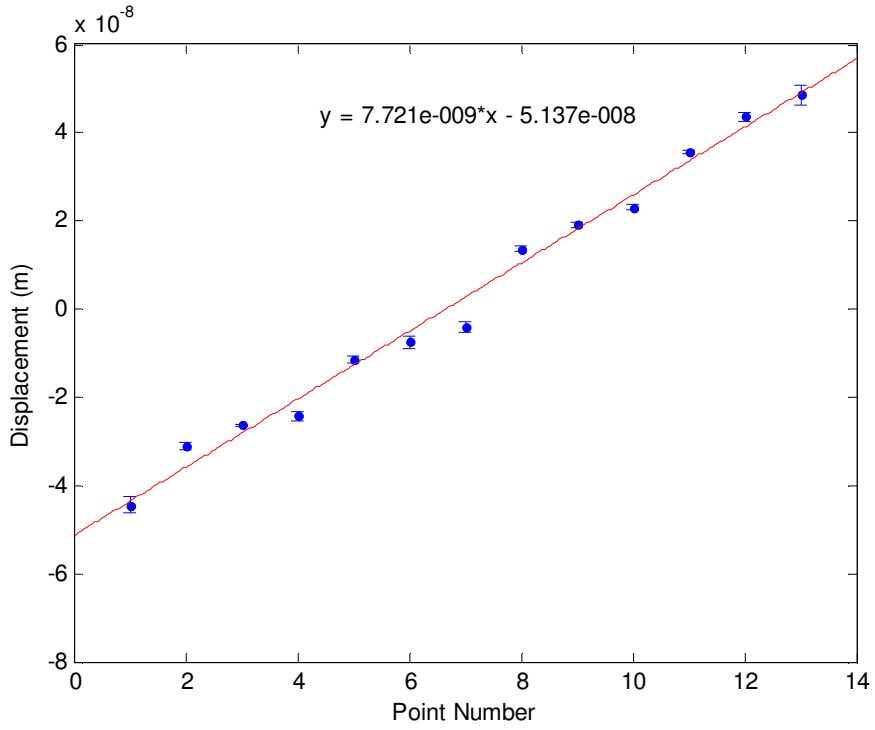
Figure 26. 200Hz Displacement at 0.6V
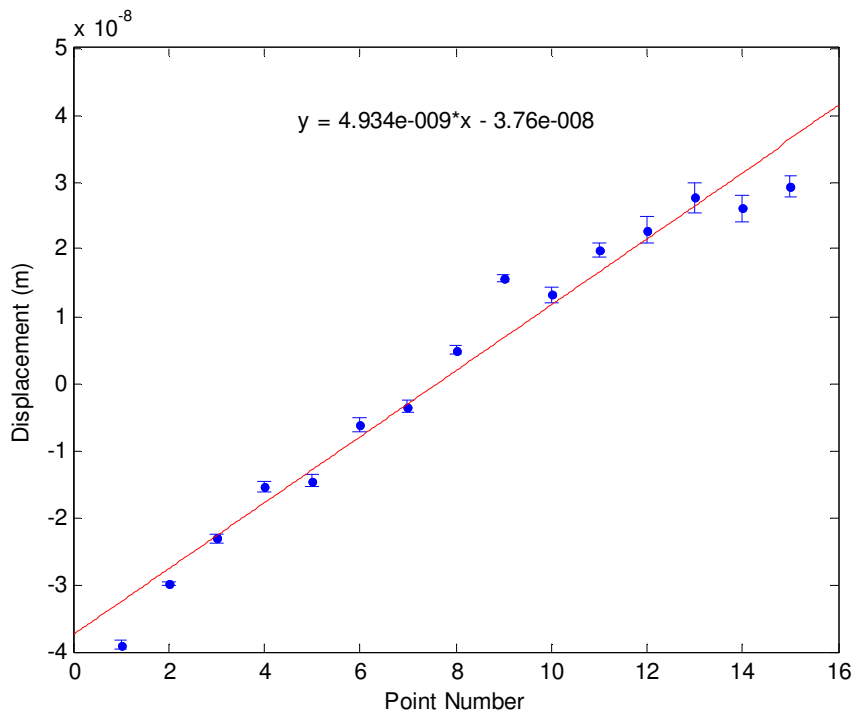
Figure 27. 200Hz Displacement at 0.4V

Summary and Discussion

The numbers for rocking and transverse displacement are summarized below in Table 4. The transverse motion was found by substituting the middle point into the linear trend line equation, and the resulting value corresponded to the transverse motion of the hemisphere. In some cases, the top and/or bottom point was too close to the edge of the hemisphere and therefore gave inaccurate results and was discarded. The maximum displacement was adjusted from the y-intercept of the linear trend line to account for these cases where differing numbers of points were used.

Table 4. Summary of Middle of Tank Results

Frequency (Hz)	Drive Level (V)	Max. Displacement (m)	Transverse Motion (m)
100	0.8	3.85e-7	1.98e-8
100	0.6	2.31e-7	1.43e-8
100	0.4	1.58e-7	1.62e-9
200	0.8	5.10e-8	6.88e-9
200	0.6	5.91e-8	2.68e-9
200	0.4	3.76e-8	1.87e-9

The results from this test had a general decrease in size of the error bars in comparison to previous tests, and a slight increase in displacements. Placing the hemisphere in the middle of the tank was beneficial, so that depth was used in all additional tests. In most cases, the decrease in drive level shows a decrease in overall motion, as predicted. While the 200Hz data does not show an exact linear trend, this could be because the noise level is much greater at 200Hz, especially at the lower drive

36

levels. Also, at 100Hz the decrease in drive level shows the displacement decreasing slightly more than a linear trend would, so both frequencies do show some amount of non-linearity. Since both frequencies show the same ratio of values for 0.4V and 0.6V, it can be assumed that the non-linearity comes from the 0.6V to 0.8V data.

The vertical motion of the hemisphere at each drive level was also calculated from the hydrophone data. The results are shown below in Table 5.

Table 5. Vertical Displacement Motion at Various Drive Levels

	100Hz	200Hz
0.8 V	3.17e-6 m	6.00e-7 m
0.6 V	2.55e-6 m	4.60e-7 m
0.4 V	1.89e-6 m	3.36e-7 m

This data shows a more constant decrease in vertical displacement as drive level decreases, but it is not completely linear. Both frequencies show a smaller decrease in displacement than a linear trend would. This data supports the theory that the decrease in drive level from 0.8V to 0.4V produces a decrease in overall motion that is not exactly linear.

CHAPTER 5

HEMI-CYLINDER TESTS

After completing all tests with the hemisphere, the responses of three different hemi-cylinders were measured. The hemi-cylinder is similar in some ways to the hemisphere, and these results could then be compared with Fan's predictions. The setup for this experiment mostly remained the same as the setup for the hemisphere, with a few changes detailed in the next section.

Setup

Three 1" diameter hemi-cylinders were tested, with lengths of 4", 6", and 8" respectively. Since Fan's results were for an infinitely long hemi-cylinder, three lengths were tested to see what extent the finite length of the hemi-cylinder was a factor. Supports were attached to the top such that they lay in the same vertical plane as the center of mass, in much the same way as the hemisphere attachments. Since the hemi-cylinders were much heavier than the hemisphere though, between four and eight supports were attached, depending on the hemi-cylinder length. The supports on the 4" length are shown in Figure 28 below.

Figure 28. Hemi-cylinder Mounting

Each hemi-cylinder was suspended 6.75" below the surface of the water from the frame in the same manner in which the hemisphere was attached. Once the depth of the hemi-cylinder and its levelness were checked, vertical scans were done with the transducer on the flat side of the hemi-cylinder. Fifteen evenly spaced points were measured along the 1" diameter of the flat side of the hemi-cylinder. Three scans were done at each frequency, 100Hz and 200Hz. Then, in the same way as with the hemisphere, measurements were taken with the large steel cylinder to account for the motion of the NIVMS assembly.

Results

The results of the scans of all three hemi-cylinders are shown in Figure 29-Figure 34. Figure 29-Figure 31 show the motion of each hemi-cylinder at 100Hz, and Figure 32-Figure 34 show the same three size hemi-cylinders at 200Hz. The x-axis represents the point number of the scan, with point 1 corresponding to the top of the hemi-cylinder increasing numbers being points further down, while the y-axis shows displacement in meters.
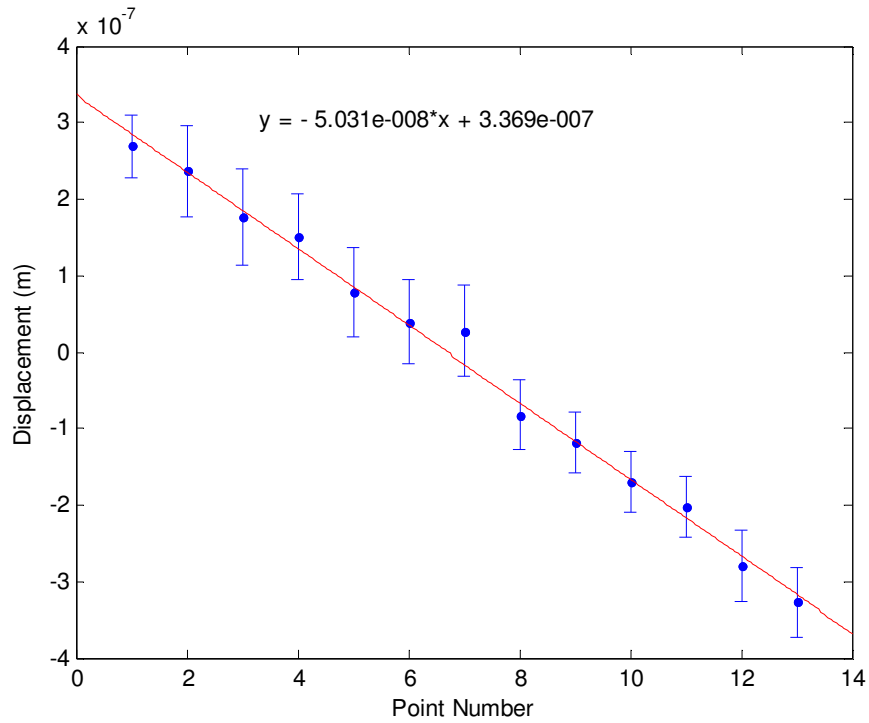
Figure 29. Displacement of 4" Hemi-cylinder at 100Hz
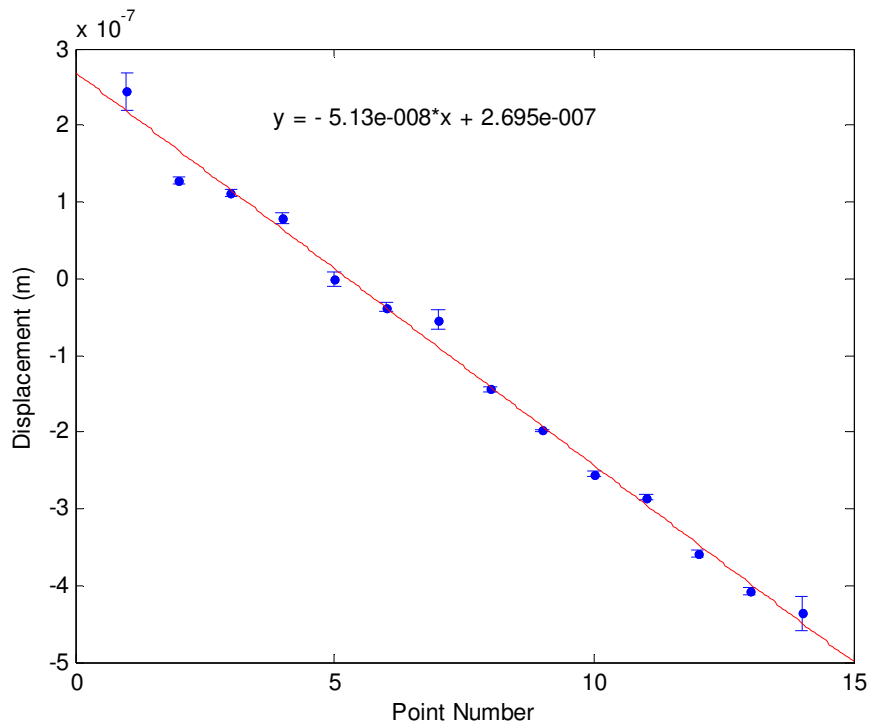
Figure 30. Displacement of 6" Hemi-cylinder at 100Hz
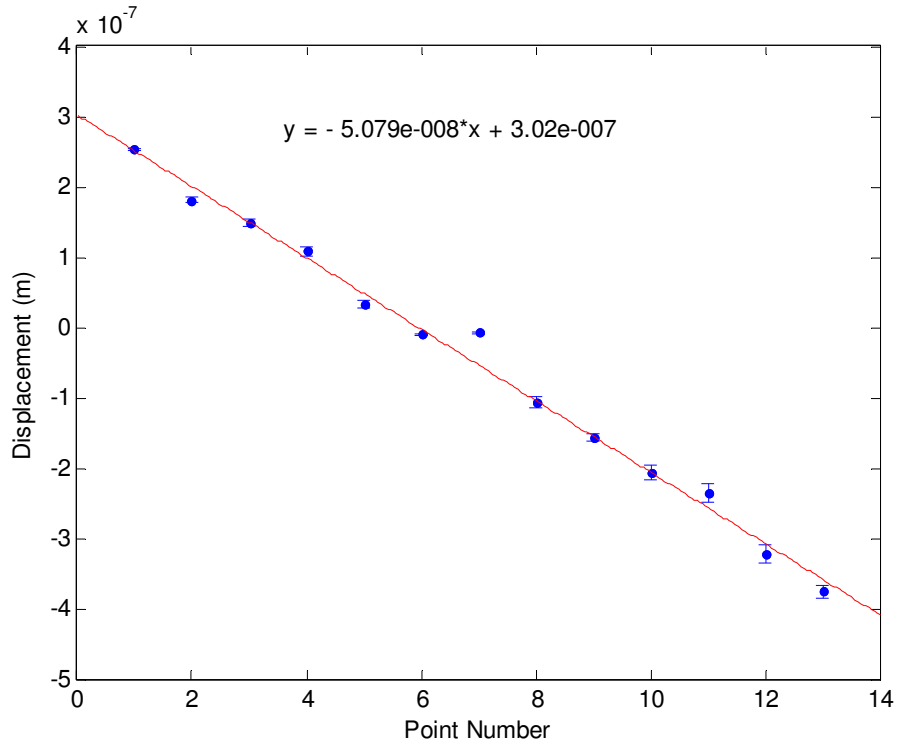
Figure 31. Displacement of 8" Hemi-cylinder at 100Hz
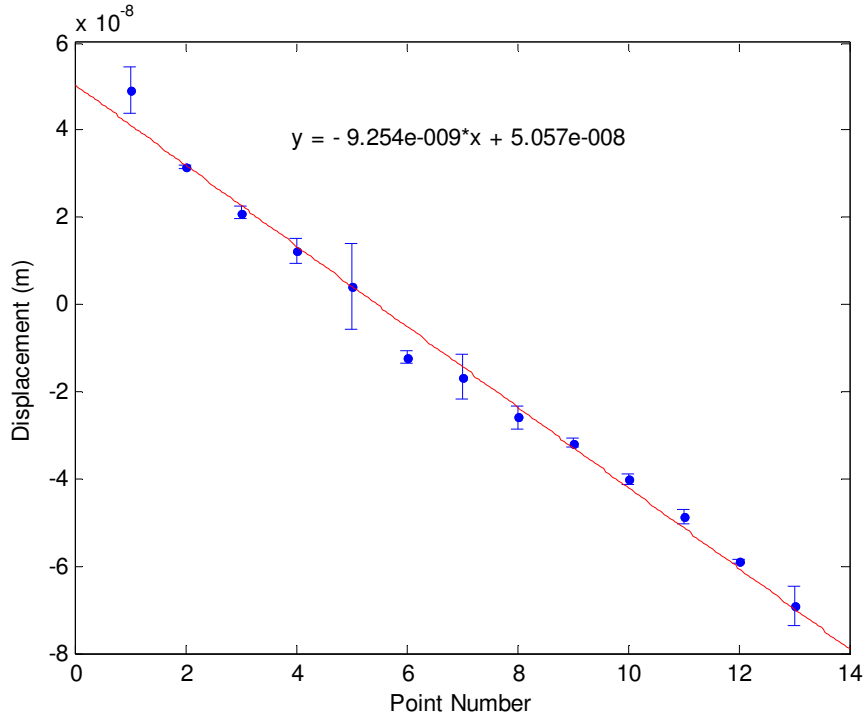
Figure 32. Displacement of 4" Hemi-cylinder at 200Hz
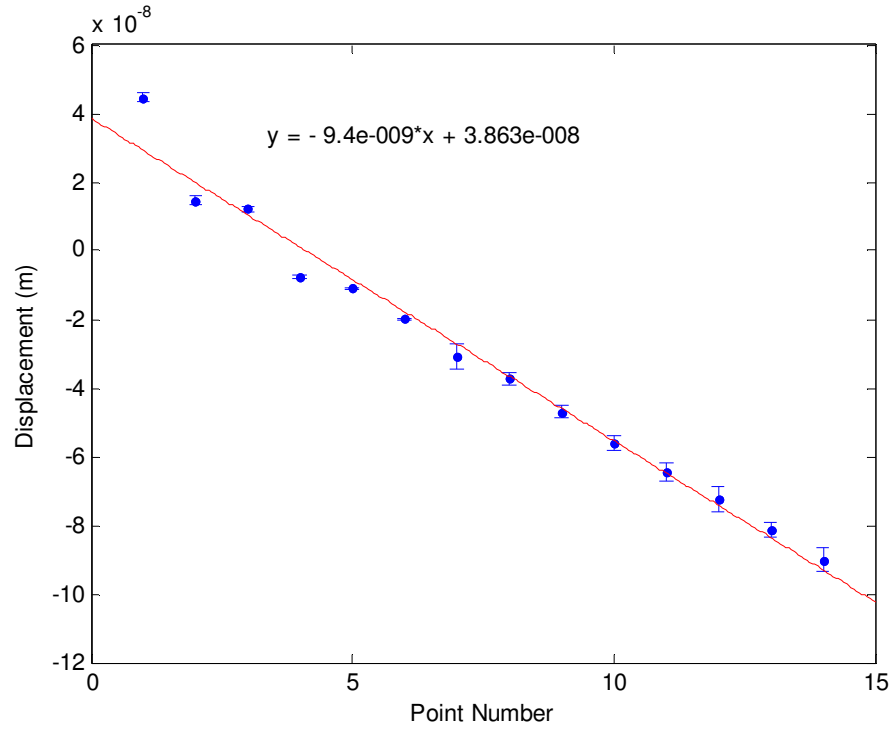
Figure 33. Displacement of 6" Hemi-cylinder at 200Hz
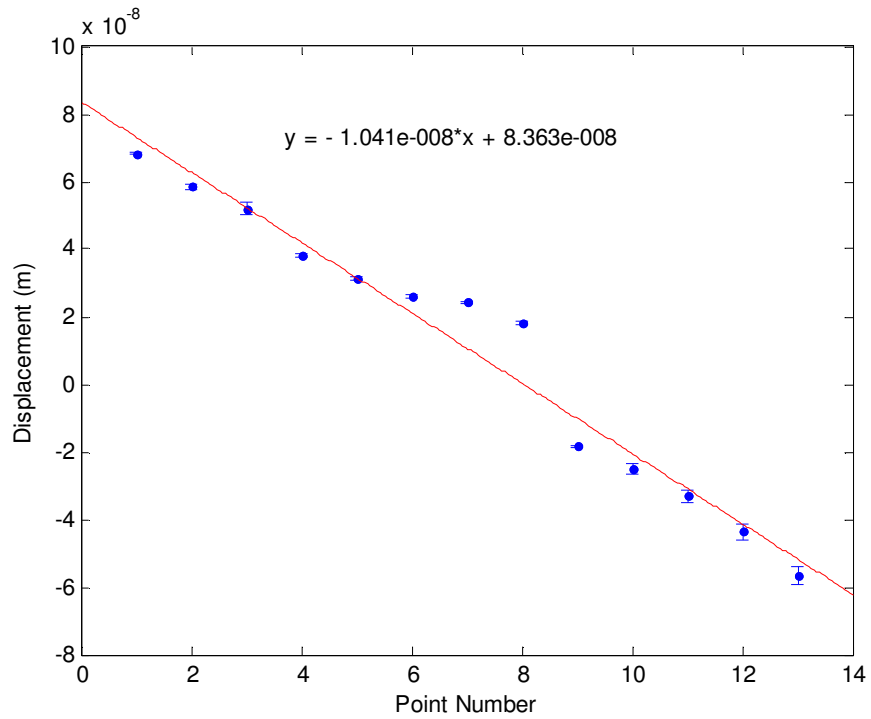
Figure 34. Displacement of 8" Hemi-cylinder at 200Hz

To summarize the previous figures, Table 6 shows the maximum displacement and transverse motion for each case. The transverse motion was found by using the linear fit curve for each case. The middle point was substituted into the equation, and the resulting value corresponded to the transverse motion of the hemi-cylinder. The maximum displacement was adjusted from the y-intercept of the linear trend line to account for different cases having differing numbers of points.

Table 6. Displacement and Transverse Motion for Each Case

Case	Max. Displacement	Transverse Motion
4" 100Hz	3.369e-7	1.53e-8
6" 100Hz	2.44e-7	8.96e-8
8" 100Hz	3.02e-7	5.35e-8
4" 200Hz	5.06e-8	1.42e-8
6" 200Hz	3.39e-8	2.72e-8
8" 200Hz	8.36e-8	0.63e-8

Discussion

While the data is not consistent across all lengths, there is not a general trend of increase or decrease in displacement as the length increases. No simple correlation between length and displacement was apparent. At 100Hz, the motion itself was also similar to the data for the hemisphere in the middle of the tank at 100Hz. The average of the data shows a rocking motion with a maximum magnitude of around 3e-7m. Differences in the displacement and transverse motion of each case could be because of slight differences in the mountings. At 200Hz, the motion is also similar to the hemisphere motion. The biggest difference between the three length hemi-cylinders is

that the longer lengths had much more consistent results. Although the average motion

from multiple trials was similar for all three lengths, the 4" length at both frequencies had

a much greater variation between trials. These results must also be compared with the

vertical motion of each hemi-cylinder, which is shown later in this section.

Comparison with Theory

In their paper on acoustic radiation torque on an irregularly shaped scatterer, Fan,

et al., show that a hemi-cylinder will rock about its center when subjected to an incident

plane wave [2]. The magnitude of the angular velocity of the rocking they find is shown

in Equation 5.

$$\omega_y = \frac{1.57*0.67\cos(\theta)(\zeta-1)}{0.67^2-1.57(0.49+0.79\zeta)(1+\zeta)}v_z \qquad \text{(Equation 5)}$$

In this equation, ω_y is the angular velocity, θ is the angle between the flat edge of the

hemi-cylinder and the z-axis (in this case $\theta = 0$), ζ is the ratio of the density of the hemi-

cylinder to the density of the water, and v_z is the velocity of the water. This equation

comes from equations for the fluid's momentum and angular momentum and the

acoustically induced-mass tensor.

For the hemi-cylinder tests, the motion of the water was found to be 0.0044 m/s at

100Hz and 0.0017 m/s at 200Hz (from the hydrophone data). Substituting those velocities

into Equation 5, the angular velocity is found to be 7.64×10^{-4} m/s at 100Hz and 2.89×10^{-4}

m/s at 200Hz. By integrating these results to get displacement, the theoretical rocking

displacements predicted by Fan, et al. are 1.2×10^{-6} m at 100Hz and 2.3×10^{-7} m at 200Hz.

These predictions are larger than the measured displacements from the tests, which

averaged to 3.2×10^{-7} m at 100Hz and 5.8×10^{-8} m at 200Hz.

Vertical Motion

As with the hemisphere, the vertical motion of each hemi-cylinder was determined. The LDV, hydrophone, and accelerometer were all used with the same methods described in Chapter 4, with a small change. The hydrophone data was the same as before, but a different formula was used to convert the motion of the water into the motion of the hemi-cylinder. This is because the two shapes behave differently when subjected to the same incident waves. The formula used for the hemi-cylinder is shown in Equation 6.

$$d = \xi \frac{2}{\frac{\rho_h}{\rho}+1} \qquad \text{(Equation 6)}$$

This formula was not dependent on length, and the measurements with the LDV and accelerometer were extremely consistent between lengths, so the results shown are for all three length hemi-cylinders. Multiple readings were taken and averaged, and the results are shown below in Table 7.

Table 7. Comparison of Three Methods of Finding Vertical Motion of Hemi-cylinder

	Displacement at 100Hz	Displacement at 200Hz
LDV	3.30e-6 m	5.92e-7 m
Hydrophone	3.66e-6 m	6.95e-7 m
Accelerometer	3.17e-6 m	5.77e-7 m

The average of the three methods gives a vertical displacement of 3.38 x 10^{-6} m at 100Hz and 6.21 x 10^{-7} m at 200Hz. The average rocking motion between the three hemi-

cylinders is 3.22 x 10^{-7} m at 100Hz and 5.82 x 10^{-8} m at 200Hz. This shows the vertical displacement being 10.5 times greater than the rocking motion at 100Hz and 10.7 times greater than the rocking motion at 200Hz. These results are similar to the results for the hemisphere case.

Sphere test

As a final test between the three methods of calculating vertical motion, the motion of a solid .75" diameter aluminum sphere was measured. There was no rocking motion in this case because the sphere was symmetric, so only the vertical motion was measured. The formula for determining the vertical motion from the hydrophone data for the hemisphere was also the formula for determining the motion of a sphere, so it was a good way to double check the results. All three measurements were taken in the same way as the measurements for the hemisphere, and the results are shown below in Table 8.

Table 8. Comparison of Three Methods of Finding Vertical Motion of Sphere

	Displacement at 100Hz	Displacement at 200Hz
LDV	3.131e-6 m	6.135e-7 m
Hydrophone	3.165e-6 m	6.003e-7 m
Accelerometer	3.541e-6 m	6.082e-7 m

The results are consistent between all three methods at 200Hz, and the LDV and hydrophone are most consistent at 100Hz. This gives more validity to the vertical motion results found for both the hemisphere and hemi-cylinder cases.

46

CHAPTER 6

CONCLUSIONS

In every case of a non-symmetric shape subjected to a plane wave, some rocking was observed. The rocking was always about the center of mass of the object, and was always much smaller in magnitude than the vertical motion. The ratio of rocking motion to vertical motion was between 7.5% and 9.8% for all cases, which is slightly smaller than Krysl's predictions of a ratio of around 13% [1]. The overall motion of the hemisphere and hemi-cylinders were also on the same order of magnitude. The results at 100Hz were generally more consistent than the results at 200Hz because the amount of noise in the data was much higher for the smaller displacement values at 200Hz. The mounting seemed to account for the greatest amount of uncertainty in the data, but even though the magnitude of the rocking motion changed somewhat between tests, it was always present and on the same order of magnitude. This supports the conclusion that the rocking itself was not an experimental artifact.

For the hemi-cylinder tests, it was found that the length of the cylinder was not directly correlated to the motion. This implies that for all the lengths tested, the system behaved as an infinite hemi-cylinder. Also, when compared with theory, the motion of the hemi-cylinders was smaller than predicted by a factor of 3-4. So while the results from these experiments do agree with theory that a rocking motion is present, they do not agree on the magnitude of that motion.

Although actual otoliths were not tested, the conclusions from the hemisphere and hemi-cylinder tests can give some insight into the motion of more complex shapes like otoliths.

REFERENCES

[1] Krysl, P., Cranford, T., Hawkins, A., and Schilt, C., Vibration of otolithlike scatterers due to low frequency harmonic wave excitation in water (Abstract). J. Acoust. Soc. Am. Volume 129, Issue 4, p. 2472 (2011);

[2] Fan, Z., Mei, D., Yang, K., Chen, Z., Acoustic radiation torque on an irregularly shaped scatterer in an arbitrary sound field, J. Acoust. Soc. Am. 124, 2727 (2008) (6 pages)

[3] Martin, J.S., Rogers, P.H., and Gray, M.D., Range discrimination in ultrasonic vibrometry: Theory and experiment, J. Acoust. Soc. Am. 130, 1735 (2011) (13 pages)